



Effect of anion and ligand ratio in self-assembled silver(I) complexes of 4-(diphenylphosphinomethyl)pyridine and their derivatives with bipyridine ligands

Fernando Hung-Low, Kevin K. Klausmeyer*, John Brannon Gary

Department of Chemistry and Biochemistry, Baylor University, Waco, TX 76798, United States

ARTICLE INFO

Article history:

Received 13 March 2008

Received in revised form 18 April 2008

Accepted 18 April 2008

Available online 24 April 2008

Keywords:

Bimetallic box

π - π interaction

Silver

Coordination modes

ABSTRACT

An efficient procedure for the synthesis of the novel bidentate ligand 4-(diphenylphosphinomethyl)pyridine (PMP-41, **1**) has been developed and its coordination behavior with Ag(I) has been studied. Reaction of the PMP-41 ligand with the silver(I) salts of tetrafluoroborate (BF_4^-), trifluoromethanesulfonate (Otf^-), and trifluoroacetate (tfa^-) produces discrete molecules and polymeric structures that depend on the varying degrees of interaction of the corresponding anion with the metal centers. When the proportion of ligand to metal is 1:1, a bimetallic box conformation is obtained with AgBF_4 and AgOtf (**2** and **5**, respectively). Varying the ratio to 2:1, a polymeric chain of bimetallic boxes is constructed when the BF_4^- salt is used (**3**). With AgTfa two distinct structural motifs are formed (**8A** and **8B**), arising from the crystallization process of using two different solvent systems. Further reaction of the $\text{AgBF}_4/\text{PMP-41}$ and $\text{AgOtf}/\text{PMP-41}$ adducts with the chelating 5,5'-dimethyl-2,2'-bipyridine or the bridging 4,4'-bipyridine ligands affords dimeric and bridged structural motifs, depending upon the coordination ability of the corresponding bipyridine fragment. Addition of the 5,5'-dimethyl-2,2'-bipyridine ligand to a solution containing AgBF_4 and PMP-41 results the capping of the silver atoms by the bipyridine fragment **4**, and the disruption of the bimetallic box in the $\text{AgOtf}(\text{PMP-41})$ structure to generate an infinite chain in a 1:1:1 ratio of the reactants **6**. As expected, the 4,4'-bipyridine acts as a bridging ligand by connecting $[\text{AgOtf}(\text{PMP-41})]_2$ molecules, which results in the formation of compound **7**. Low-temperature luminescence spectra were also collected for all compounds and are compared.

© 2008 Elsevier B.V. All rights reserved.

1. Introduction

Pyridyl-substituted phosphines [1–5], which were first reported more than 60 years ago, have been extensively used in metal ion coordination chemistry for their ease of functionalization and the electronic properties that they impart to metal complexes used for catalysis purposes [6–15]. The presence of both hard and soft-donating atoms make it easy to coordinate as a multidentate ligand, as seen for the series of 2-(phosphinomethyl)pyridyl of the type $\text{PPh}_x\text{CH}_2\text{py}_{3-x}$ ($x = 0, 1, 2$). From this family of ligands, the coordination chemistry of the 2-(diphenylphosphinomethyl)pyridine [16–20] ($\text{PPh}_2\text{CH}_2\text{py}$, PMP-21) and the phenylphosphino-bis-2-methylpyridyl [21,22] ($\text{PPh}(\text{CH}_2\text{py}_2)_2$, PMP-22) have been widely studied in our group using different Ag(I) salts of both interacting and non-interacting anions. Interesting structural variations within the series $\text{AgX}/\text{PPh}_x\text{CH}_2\text{py}_{3-x}$ ($x = 1$ or 2) result from the different coordination modes of the anions, as well as supramolecular interactions such as hydrogen-bonding, π - π stacking, electrostatic and van der Waals interactions, which are determinant in the construction of such coordinative structures

[23–27]. In this paper we report the synthesis and coordinative behavior of 4-(diphenylphosphinomethyl)pyridine (Fig. 1) with different silver salts. No reports have been published that involve the use of this bidentate ligand, except for the structurally similar related 4-pyridyldiphenylphosphine ligand [28], that have been seen to form bimetallic complexes with transition metals like W, Fe, Ru, and Rh [29–31]. The incorporation of a methyl group between the P atom and the pyridyl group increases the variety of conformations for the ligand. This structural feature has allowed the synthesis of discrete molecules and very complex coordination polymers of various silver(I) salts. Despite the variety of coordinative environments encountered around the metal centers, excepting one of all metal complexes reported herein present one structural feature in common in that the phosphine ligand coordinates head-to-tail, P–Ag–N, which accounts for the symmetric coordinating mode of the PMP-41 ligand.

The preparation of mixed-ligand complexes has also been achieved by addition of the 5,5'-dimethyl-2,2'-bipyridine or 4,4'-bipyridine ligands to reaction mixtures containing equivalent amounts of AgX ($X = \text{BF}_4^-$ or Otf^-) and PMP-41. The use of a predominantly chelating bipyridine ligand [32,33] and a rigid connector with two binding sites in a divergent fashion [34–37], allowed the formation of polymeric structures and multidimensional

* Corresponding author. Fax: +1 254 710 4272.

E-mail address: Kevin_Klausmeyer@baylor.edu (K.K. Klausmeyer).

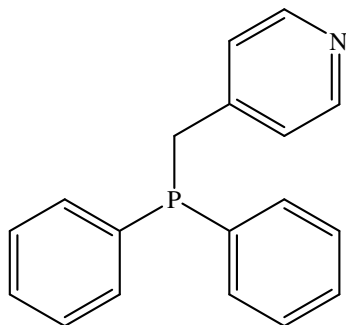


Fig. 1. Structure of PMP-41 ligand.

coordination networks, most of which were obtained by controlling functionality of the corresponding ligand, ratio of reactants or solvent system. Herein, we describe the variations in the coordinative environments of the silver(I) centers that results from the coordination of the bipyridine ligand to the corresponding AgX:PMP-41 complex, and the changes in luminescence properties exhibited from the different Ag–P interactions in the presence of a bipyridine ligand. The **PMP-nm** naming convention that we have adopted in here and in different reports, allows for simplicity in discussion of these phosphinomethylpyridines, as there are many substitutions that can be made and systematic nomenclature can be cumbersome. As such, **PMP** indicates the phosphinomethylpyridine ligands, where **n** is the position of substitution on the pyridyl ring and **m** is the number of substitutions by methylpyridine on the phosphorus.

2. Experimental

2.1. General remarks

All syntheses and handling were carried out under a nitrogen atmosphere using a Schlenk line and standard Schlenk techniques. All silver salt reagents were stored in an inert-atmosphere glove-box; solvents were distilled under nitrogen from the appropriate drying agent immediately before use. *n*-Butyllithium, chlorodiphenylphosphine, 5,5'-dimethyl-2,2'-bipyridine, and 4,4'-bipyridine were purchased from Aldrich and used as received. Silver(I) tetrafluoroborate, silver(I) trifluoromethanesulfonate, and silver(I) trifluoroacetate were purchased from Strem Chemicals Inc. and used as received. ¹H, ³¹P and variable-temperature ³¹P NMR spectra were recorded at 360.13 MHz with a Bruker Spectrospin 300 MHz spectrometer. Elemental analyses were performed by Atlantic Microlabs Inc. in Norcross, Georgia. Excitation and emission spectra were recorded with an Instruments S.A. Inc. Fluoromax-2 model spectrometer using band pathways of 5 nm for both excitation and emission and are presented uncorrected.

2.2. Synthesis

2.2.1. Synthesis of 4-(diphenylphosphinomethyl)pyridine, PMP-41 (**1**)

n-Butyllithium (17 mmol, 5.86 mL, 2.9 M in hexane) was added over a period of 10 min to 4-picoline (17 mmol, 1.67 mL) in dry THF (20 mL) at –41 °C. After stirring for 1 h, the mixture was added dropwise to a solution of chlorodiphenylphosphine (3.0 g, 17 mmol) in dry THF (20 mL) at –84 °C. Water (20 mL) was then added over 10 min and the mixture stirred for 30 min. The product was obtained by first extracting with 0.3 N HCl(aq), then neutralizing with a NaHCO₃ solution, and extracting with dichloromethane. The solvent and any un-reacted 4-picoline were removed under vacuum (oil pump) and a light yellow solid resulted with purity

>97% in 78% yield. If necessary, purification of the ligand can be achieved by precipitation with CH₂Cl₂/hexanes mixtures. ¹H NMR (CDCl₃, 298 K) δ: 3.40 (s, 2H), 6.96 (m, 2H), 7.39 (m, 10H), 8.41 (d, 2H). ³¹P NMR (CDCl₃, 298 K) δ: (–8.81, s).

2.2.2. Synthesis of [AgBF₄(PMP-41)(CH₃CN)₂]₂ (**2**)

To a stirred solution of AgBF₄ (0.077 g, 0.396 mmol) in CH₃CN (5 mL) was added **1** (0.109 g, 0.396 mmol) in CH₃CN (5 mL). The resulting solution was allowed to stir for 5 min and then dried in vacuo to leave a brownish solid. This was then re-dissolved in a small amount of CH₂Cl₂ and precipitated with ether to obtain compound **2** as a white powder upon drying in 57% (0.125 g, 0.225 mmol) yield. Colorless blocks were obtained by slow diffusion of ether into a CH₃CN solution of **2** at 5 °C. ¹H NMR (CD₃CN, 298 K) δ: 3.88 (m, 2H), 7.05 (m, 2H), 7.72 (m, 10H), 8.09 (m, 2H). ³¹P NMR (CD₃CN, 243 K) δ: 15.7, d. *Anal. Calc.* for C₂₂H₂₂AgBF₄N₃P (554.08): C, 46.82; H, 3.73; N, 5.46. Found: C, 46.91; H, 3.65; N, 5.25.

2.2.3. Synthesis of AgBF₄(PMP-41)₂ (**3**)

This reaction used 2 equiv. of **1** (0.222 g, 0.801 mmol) in CH₃CN (5 mL) added to 1 equiv. of AgBF₄ (0.078 g, 0.402 mmol) in CH₃CN (5 mL). After stirring for 5 min, the solution was dried in vacuo and a light yellow solid was obtained. This was then dissolved in a small amount of CH₂Cl₂ and precipitated with ether to obtain compound **3** as a white solid upon drying in 58% (0.175 g, 0.233 mmol) yield. Crystallization formed colorless blocks obtained by slow diffusion of ether into a CH₃CN solution of **3** at 5 °C. ¹H NMR (CD₃CN, 298 K) δ: 3.78 (m, 2H), 6.85 (m, 2H), 7.57 (m, 10H), 8.07 (m, 2H). ³¹P NMR (CD₃CN, 243 K) δ: 9.01, d. *Anal. Calc.* for C₃₆H₃₂AgBF₄N₂P₂ (748.87): C, 57.71; H, 4.30; N, 3.94. Found: C, 57.24; H, 4.12; N, 4.34.

2.2.4. Synthesis of [AgBF₄(PMP-41)(5,5'-dimethyl-2,2'-bipyridine)]₂ (**4**)

This reaction used 1 equiv. of **1** (0.110 g, 0.402 mmol) in CH₃CN (5 mL) added to 1 equiv. of AgBF₄ (0.079 g, 0.406 mmol) in CH₃CN (5 mL). After stirring for 5 min, a solution of 5,5'-dimethyl-2,2'-bipyridine (0.073 g, 0.396 mmol) in CH₃CN (5 mL) was added to the reaction mixture. After stirring for 10 min, a white solid precipitated, which was then isolated by removing the solvent. Upon evaporation, a light yellow powder was obtained in 69% yield (0.185 g, 0.282 mmol). Crystallization formed colorless blocks obtained by slow diffusion of hexane into a CH₂Cl₂ solution of **4** at 5 °C. ¹H NMR ((CD₃)₂CO, 298 K) δ: 2.47 (s, 6H), 4.13 (m, 2H), 7.23 (m, 2H), 7.63 (m, 6H), 7.95 (m, 4H), 8.05 (m, 2H), 8.28 (m, 2H), 8.45 (m, 2H), 8.50 (s, 2H). ³¹P NMR ((CD₃)₂CO, 243 K) δ: 11.03, d. *Anal. Calc.* for C₃₀H₂₈AgBF₄N₃P₁ (656.22): C, 54.01; H, 4.30; N, 6.40. Found: C, 53.97; H, 4.33; N, 6.25.

2.2.5. Synthesis of AgOtf(PMP-41) (**5**)

To a stirred solution of AgOtf (0.109 g, 0.399 mmol) in CH₃CN (5 mL) was added **1** (0.109 g, 0.399 mmol) in CH₃CN (5 mL). The resulting solution was allowed to stir for 5 min and then dried in vacuo to leave an off-white powder. The compound was re-crystallized with CH₂Cl₂/ether solutions upon drying in 83% (0.177 g, 0.331 mmol) yield. Colorless blocks were obtained by slow diffusion of ether into a CH₃CN solution of **5** at 5 °C. ¹H NMR (CD₃CN, 298 K) δ: 3.88 (d, 2H), 7.03 (m, 2H), 7.63 (m, 10H), 8.09 (m, 2H). ³¹P NMR (CD₃CN, 243 K) δ: 15.75, d. *Anal. Calc.* for C₁₉H₁₆AgF₃NO₃PS (534.23): C, 42.72; H, 3.02; N, 2.62. Found: C, 42.92; H, 2.86; N, 2.53.

2.2.6. Synthesis of AgOtf(PMP-41)(5,5'-dimethyl-2,2'-bipyridine) (**6**)

To a stirred solution of AgOtf (0.107 g, 0.392 mmol) in CH₃CN (5 mL) was added **1** (0.109 g, 0.399 mmol) in CH₃CN (5 mL). The

resulting solution remained clear and colorless, and after stirring for 5 min a solution of 5,5'-dimethyl-2,2'-bipyridine (0.073 g, 0.396 mmol) in CH₃CN (5 mL) was added to the mixture. After stirring for 10 min, the solution was dried in vacuo and a light yellow solid was obtained. This was then washed several times with acetone to obtain compound **6** as a white solid upon drying in 65% (0.183 g, 0.255 mmol) yield. Colorless block crystals were obtained by slow diffusion of hexane into a CH₂Cl₂ solution of **6** at 5 °C. ¹H NMR (CD₃CN, 298 K) δ: 2.13 (s, 6H), 3.89 (d, 2H), 7.02 (m, 2H), 7.61 (m, 6H), 7.77 (m, 4H), 7.94 (m, 2H), 8.21 (m, 4H), 8.35 (s, 2H). ³¹P NMR (CD₃CN, 243 K) δ: 18.39, d. *Anal. Calc.* for C₃₁H₂₈AgF₃N₃O₃PS (718.46): C, 51.82; H, 3.93; N, 5.85. Found: C, 51.58; H, 3.94; N, 5.93.

2.2.7. Synthesis of [AgOtf(PMP-41)](4,4'-bipyridine)_{1/2} (**7**)

This reaction used 1 equiv. of **1** (0.110 g, 0.401 mmol) in CH₃CN (5 mL) added to 1 equiv. of AgOtf (0.109 g, 0.399 mmol) in CH₃CN (5 mL). This was stirred for 5 min, and then a solution of 4,4'-bipyridine (0.031 g, 0.201 mmol) in CH₃CN (5 mL) was added to the solution. This mixture was stirred for 10 min, and the solvent was removed in vacuo to leave a white powder in 73% isolated yield (0.178 g, 0.097 mmol). Colorless block crystals were obtained by slow diffusion of hexane into a solution of **8** in CH₂Cl₂ at 5 °C. ¹H NMR (CD₃CN, 298 K) δ: 3.82 (m, 2H), 6.99 (m, 2H), 7.62 (m, 18H), 8.73 (m, 2H). ³¹P NMR (CD₃CN, 243 K) δ: 13.06, br, s. *Anal. Calc.* for C₇₂H₆₀Ag₃F₉N₆O₉P₃S₃ (1836.96): C, 47.08; H, 3.29; N, 4.57. Found: C, 47.23; H, 3.32; N, 4.60.

2.2.8. Synthesis of Agtfa(PMP-41) (**8A** and **8B**)

This reaction used **1** (0.109 g, 0.398 mmol) in CH₃CN (5 mL) added to a stirred solution of Agtfa (0.880 g, 0.398 mmol) in CH₃CN (5 mL). After stirring for 5 min a white solid precipitated out of the solution to leave a fluffy off-white powder upon evaporation of the solvent. The compound was purified by washing with CH₃CN since it is only slightly soluble in the solvent. Upon drying the compound, the product was obtained in 81% (0.160 g, 0.322 mmol) yield. Colorless blocks of **8A** were obtained by slow diffusion of ether into a CH₃CN solution of the compound at 5 °C, and colorless blocks of **8B** by layering ether into a DMF solution of the same solid. ¹H NMR (CH₃OD, 298 K) δ: 3.96 (d, 2H), 7.17 (m, 2H), 7.60 (m, 6H), 7.85 (m, 4H), 8.09 (m, 2H). ³¹P NMR (CH₃OD, 243 K) δ: 15.77 br, d. *Anal. Calc.* for C₂₀H₁₆AgF₃N₁O₂P (498.18): C, 48.22; H, 3.24; N, 2.81. Found: C, 48.03; H, 3.24; N, 2.78.

3. Results and discussion

3.1. General characterizations

3.1.1. Synthesis and NMR spectra

The novel 4-(diphenylphosphinomethyl)pyridine ligand, synthesized by a procedure similar to that reported for the PMP-21 ligand [19,20], is made by the reaction of the corresponding 4-lithiomethylpyridine with Ph₂PCl at low temperature to afford **1** in high yield and purity. Care must be taken during the formation of the pyridyllithium prior to the addition to the phosphorus halide, since it was observed that this stage of the reaction is responsible for the formation of several unidentified phosphine oxide byproducts. Experimental observations indicate that intermediates of the reaction are sensitive to parameters such as temperature, addition rate, and solvent. High temperatures, rapid addition rates, and non-polar solvents, such as ether, reduce dramatically the formation of **1**, and enhance the production of other phosphine compounds. Decomposition of **1** is observed when exposed to air, observing the transition from a light to dark yellow solid. By refrigeration under an inert atmosphere, compound **1**

can be preserved for a period up to 3 months. Pure **1** can be separated, if necessary, from its decomposition products by precipitation of the ligand with CH₂Cl₂/hexanes mixtures. ¹H and ³¹P NMR spectra of **1** in CDCl₃ verify the formation of the PMP-41 ligand, with a phosphorus singlet at –8.81 ppm, which is in the region expected for aromatic-substituted phosphines.

The reaction under ambient conditions in an inert atmosphere of three different silver(I) salts (BF₄[–], Otf[–], or tfa[–]) with **1** affords compounds **2**, **5**, **8A**, and **8B** in a 1:1 ligand to metal ratio, and compound **3** in a 2:1 proportion. Under the same conditions, reaction of 1 equiv. of 5,5'-dimethyl-2,2'-bipyridine in a reaction mixture containing AgBF₄ and PMP-41 yields compound **4**. Reaction of the AgOtf/PMP-41 adduct with 1 equiv. of 5,5'-dimethyl-2,2'-bipyridine and 1/2 equiv. of 4,4'-bipyridine yields compounds **6** and **7** respectively. No further reaction of the [Agtfa(PMP-41)]₂ complex with any of the bipyridine ligands is observed, due to corroborated evidences that demonstrate the silver centers are sterically and electronically crowded when using a coordinating anion like tfa [20]. Upon coordination, all of the silver compounds reported herein are stable in air and room temperatures, with little sign of decomposition within several hours upon exposure to light. In solution, the metal compounds tend to undergo decomposition to form an oily black product.

The ¹H and ³¹P NMR spectra of all compounds were collected in CD₃CN, excepting **4** and **8**, which were recorded in deuterated acetone and methanol respectively, due to the solubility of each compound. The ¹H NMR spectra of compounds **2–8** are, as expected, generally similar. At room temperature, ³¹P NMR spectra show a doublet of broad peaks and only in compound **7** a broad singlet owing to the phosphorous-silver coupling. This indicates at least some degree of coordination of the ligand to silver in room temperature solutions, though the process does appear to be dynamic on the NMR time scale. Variable temperature ³¹P NMR were collected at –30 °C for all compounds to observe the dissociation of the Ag–P bond. In most of the compounds it was observed a sharpening of the doublet peaks, and in the case of a broad singlet, the corresponding splitting into doublet peaks. The coupling of the separate isotopes of Ag was not observed in any of the metal complexes.

3.2. Description of the crystal structures

Single X-ray diffraction data were collected on crystals with approximate dimensions of 0.280 × 0.180 × 0.120 mm for **2**, 0.250 × 0.150 × 0.140 mm for **3**, 0.361 × 0.231 × 0.152 mm for **4**, 0.190 × 0.120 × 0.110 mm for **5**, 0.220 × 0.170 × 0.160 mm for **6**, 0.210 × 0.164 × 0.157 mm for **7**, 0.200 × 0.120 × 0.100 mm for **8**, and 0.294 × 0.216 × 0.214 mm for **8B**. Data were collected at 110 K on a Bruker X8 Apex using Mo K α radiation (λ = 0.71073 Å). All structures were solved by direct methods after correction of the data using SADABS [38,39]. Details of the crystal parameters, data collection, and refinement are summarized in Tables 1 and 2. The molecular structure of the compounds is displayed in Figs. 2–10. Summary of selected bond lengths, angles, and interatomic distances are given in Tables 3 and 4. All data were processed using the Bruker AXS SHELXTL software, version 6.10 [40]. Hydrogen atoms were placed in calculated positions and all non-hydrogen atoms were refined anisotropically, unless specified. Compound **3** has a volume of 998 Å³/unit cell volume, which contains several solvent molecules. We were unable to satisfactorily model these solvent molecules and therefore they were removed from the structure using the SQUEEZE procedure implemented in PLATON [41].

3.2.1. Structure of compound **2**

The coordination of the silver centers in compound **2** is characterized by a pair of head-to-tail coordinated PMP-41 ligands bound

Table 1
Crystallographic data for complexes 2–5

Compound	2	3	4	5
Empirical formula	C ₄₈ H ₅₀ Ag ₂ B ₂ F ₈ N ₈ P ₂	C ₁₁₆ H ₁₀₈ Ag ₃ B ₂ F ₈ N ₁₀ P ₆	C ₆₄ H ₆₄ Ag ₂ B ₂ C ₈ F ₈ N ₆ P ₂	C ₁₉ H ₁₆ AgF ₃ NO ₃ PS
Formula mass	1190.26	2325.17	1652.11	534.23
<i>a</i> (Å)	8.6060(9)	18.203(3)	11.4103(19)	8.7089(4)
<i>b</i> (Å)	10.9368(11)	28.542(4)	13.537(2)	11.1276(5)
<i>c</i> (Å)	14.4667(16)	23.783(3)	13.744(2)	11.2426(5)
α (°)	80.640(5)	90	92.193(8)	87.816(3)
β (°)	79.864(5)	104.008(7)	113.884(8)	83.551(3)
γ (°)	81.467(5)	90	111.568(7)	70.806(3)
<i>V</i> (Å ³)	1312.4(2)	11989(3)	1760.9(5)	1022.43(8)
<i>Z</i>	1	4	1	2
Crystal system	triclinic	monoclinic	triclinic	triclinic
Space group	<i>P</i> $\bar{1}$	<i>C</i> 2/ <i>c</i>	<i>P</i> $\bar{1}$	<i>P</i> $\bar{1}$
<i>T</i> [K]	110(2)	110(2)	110(2)	110(2)
<i>D</i> _{calc} (g cm ⁻³)	1.506	1.288	1.558	1.735
μ (mm ⁻¹)	0.877	0.626	0.970	1.213
2 θ _{max} (°)	25.00	26.37	26.47	26.44
Reflections measured	38 810	56 690	37 315	9971
Reflections used (<i>R</i> _{int})	4607 (0.0408)	12 276 (0.0480)	7167 (0.0364)	4151 (0.0421)
Restraints/parameters	10/356	0/656	0/417	0/262
<i>R</i> ₁ [<i>I</i> > 2 σ (<i>I</i>)]	0.0346	0.0412	0.0247	0.0385
<i>wR</i> ₂ [<i>I</i> > 2 σ (<i>I</i>)]	0.0877	0.1128	0.0578	0.0831
<i>R</i> (<i>F</i> _o ²) (all data)	0.0373	0.0556	0.0279	0.0498
<i>R</i> _w (<i>F</i> _o ²) (all data)	0.0911	0.1186	0.0599	0.0905
Goodness-of-fit (GOF) on <i>F</i> ²	1.041	1.083	1.025	1.030

Table 2
Crystallographic data for complexes 6–8

Compound	6	7	8A	8B
Empirical formula	C ₃₁ H ₂₈ AgF ₃ N ₃ O ₃ PS	C ₇₂ H ₆₀ Ag ₃ F ₉ N ₆ O ₉ P ₃ S ₃	C ₂₂ H ₁₉ AgF ₃ N ₂ O ₂ P	C ₂₀ H ₁₆ AgF ₃ NO ₂ P
Formula mass	718.46	1836.96	539.23	498.18
<i>a</i> (Å)	17.163(4)	10.7913(7)	7.7386(8)	24.3039(11)
<i>b</i> (Å)	10.560(3)	15.3140(9)	27.933(3)	9.1146(4)
<i>c</i> (Å)	17.885(3)	24.5005(15)	10.4527(9)	17.9687(8)
α (°)	90	74.212(2)	90	90
β (°)	112.344(9)	89.7100(10)	97.830(3)	108.306(2)
γ (°)	90	75.7750(10)	90	90
<i>V</i> (Å ³)	2998.1(11)	3768.4(4)	2238.4(4)	3779.0(3)
<i>Z</i>	4	2	4	8
Crystal system	monoclinic	triclinic	monoclinic	monoclinic
Space group	<i>P</i> 2 ₁ / <i>n</i>	<i>P</i> $\bar{1}$	<i>P</i> 2 ₁ / <i>c</i>	<i>C</i> 2/ <i>c</i>
<i>T</i> (K)	110(2)	110(2)	110(2)	110(2)
<i>D</i> _{calc} (g cm ⁻³)	1.592	1.619	1.600	1.751
μ (mm ⁻¹)	0.852	1.000	1.017	1.196
2 θ _{max} (°)	27.18	25.73	26.43	26.46
Reflections measured	27 095	53 351	22 429	17 515
Reflections used (<i>R</i> _{int})	6640 (0.0524)	14 070 (0.0598)	4585 (0.0494)	3824 (0.0468)
Restraints/parameters	19/424	0/946	0/281	0/253
<i>R</i> ₁ [<i>I</i> > 2 σ (<i>I</i>)]	0.0422	0.0367	0.0364	0.0333
<i>wR</i> ₂ [<i>I</i> > 2 σ (<i>I</i>)]	0.0922	0.0750	0.0716	0.0747
<i>R</i> (<i>F</i> _o ²) (all data)	0.0584	0.0563	0.0523	0.0469
<i>R</i> _w (<i>F</i> _o ²) (all data)	0.1022	0.0849	0.0783	0.0820
Goodness-of-fit (GOF) on <i>F</i> ²	1.023	1.049	1.043	1.033

to the two symmetry equivalent silvers. This bimetallic box is the common unit relating all structures with PMP-41, where the *para* substitution of the nitrogen on the pyridyl ring makes it ideal for this type of conformation. In this arrangement the pyridyl π -systems of the opposing ligands are conveniently oriented to interact with one another, forming a rather rectangle. A thermal ellipsoid plot of the discrete molecule of **2** is presented in Fig. 2, and selected bond lengths and angles are given in Table 3. Adjacent molecules are perfectly aligned in one dimension down the crystallographic *b*-axis, as observed in the packing structure of **2** shown in Fig. 3, with no apparent π - π interactions between the aromatic rings. The geometry around the metal centers consists of a distorted tetrahedron with two CH₃CN molecules completing the coordination sphere of the Ag atoms. The angles around Ag1 range between

89.96(11) and 125.55(8)°, and the Ag–P and Ag–N distances fall in the range of reported values. The angle formed between the P and the pyridyl arm of the PMP-41 ligand allows for an easy approach of the N-donor atom to the metal center, with a value of 110.54(19)° for C(2)#1–C(1)–P(1). The BF₄ anion is disordered about the position of the boron, and is refined isotropically. The center of the bimetallic box lies on a crystallographic inversion center. (See Table 5)

3.2.2. Structure of compound 3

The molecular structure of compound **3** consists of a polymeric array in a 2:1 ligand to metal ratio, which results from the substitution of the two CH₃CN molecules observed in **2**, by another equivalent of PMP-41 to afford the polymeric chain. A view of

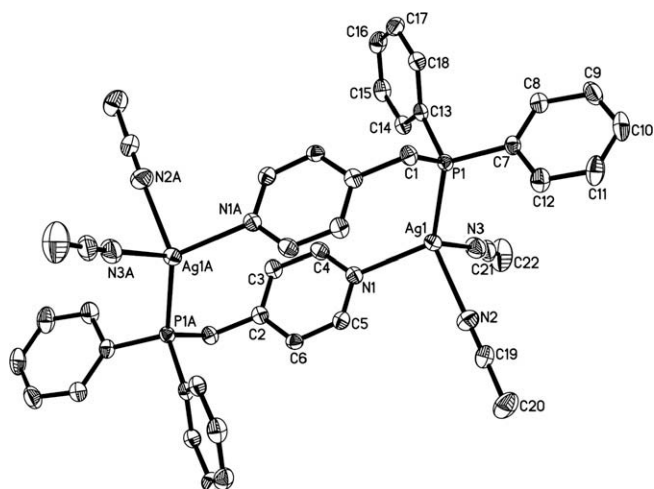


Fig. 2. Thermal ellipsoid of the cationic portion of **2** with an atomic numbering scheme. Ellipsoids are shown at the 50% level. Hydrogen atoms and two CH_3CN molecules have been removed for clarity.

the infinite chain of this structure and the thermal ellipsoid plot of the unique portion of **3** are shown in Fig. 4. The metal centers are repeated in one dimension, each one constituting an axis of two bimetallic boxes which are in a zigzag conformation. The planes of two consecutive bimetallic boxes present an approximate angle of 90° , from which it can be seen as an infinite ladder. Each Ag atom is coordinated to two N and P atoms belonging to four different PMP-41 ligands. A distorted tetrahedral geometry is observed for the silver ions in compound **3**, with little variances in the angles when moving from one metal center to another. The Ag–P distances display an average value of $2.4549(9)$ Å, which is considerably longer than the reported value of $2.3701(8)$ Å for Ag(1)–P(1) in compound **2**. This observation reflects the increase in electron donation to the silver atom in compound **3**, when another pyridyl group of a PMP-41 ligand is coordinated to the metal center, thus resulting in elongated distances due to the weakening of the Ag–P interactions.

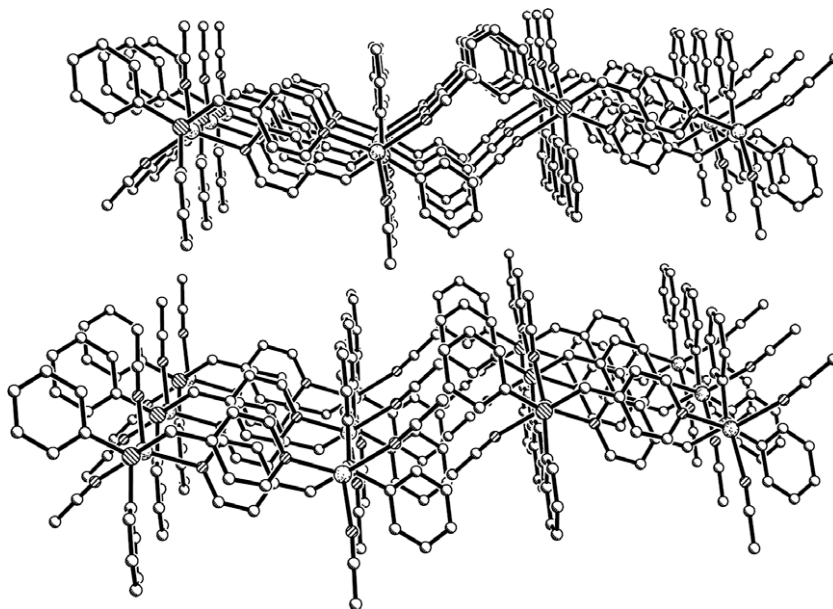


Fig. 3. Packing structure of complex **2** showing the 3-D growth of the molecule. H atoms, tetrafluoroborates, and all the solvent molecules have been removed for clarity.

3.2.3. Structure of compound **4**

Given the labile nature of the two CH_3CN molecules coordinated to the silver centers in compound **2**, design of mixed-ligand complexes using additional electron donating ligands appeared to be feasible. Reaction of the bidentate 5,5'-dimethyl-2,2'-bipyridine with a solution containing AgBF_4 and PMP-41 in a 1:1:1 ratio of the reactants, gave rise to the formation of compound **4** (Fig. 5). As expected, the chelating bipyridine preferentially binds the silver(I) cation, displacing the solvent molecules from its coordination sphere to form a discrete bimetallic molecule. The metal centers are in distorted tetrahedral environments with angles ranging between $71.58(5)$ and $133.61(4)^\circ$. The high deformation of the tetrahedral bond angles in this compound results from the small bite angle of the coordinated bipyridine ligand. The aromatic rings of the bipyridine fragment are twisted from planarity at an angle of $14.1(1)^\circ$. The Ag–P and Ag–N distances are comparable with those reported for compound **2**, and therefore no large variances in electron donation to the Ag centers is obvious by substituting the CH_3CN molecules with bipyridine ligands. Molecules of compound **4** display weak π – π interactions in the crystal system between the aromatic rings of the bipyridine ligands. The distance between the planes of the π -systems averages around 3.6 Å from one molecule to the next in the crystal structure, as shown in the supplementary material (Fig. S1). The center of the molecule lies on a crystallographic inversion center.

3.2.4. Structure of compound **5**

The X-ray crystal structure of compound **5** reveals the triflate anion playing an integral part in deciding the geometry of the silver ions and the connectivity with adjacent molecules. A thermal ellipsoid plot of the molecular structure of **5** is shown in Fig. 6b, where the bimetallic box motif is conserved, based upon the symmetric bidentate ligand. Compound **5** consists of a polymeric structure in a 1:1 ligand to metal ratio, where the bimetallic boxes are held together by the triflate anions through a single oxygen, thus acting as a bridging connector between the silver atoms (Fig. 6a) [42–46]. Although the sulfonate oxygen is connected to two identical atoms, the bridging is quite asymmetric, as denoted by the Ag1–O distances varying from $2.489(2)$ to 2.607 Å with the longer value represented by the bridging contact. The molecular structure of this polymeric chain is obtained by growing the unique part of

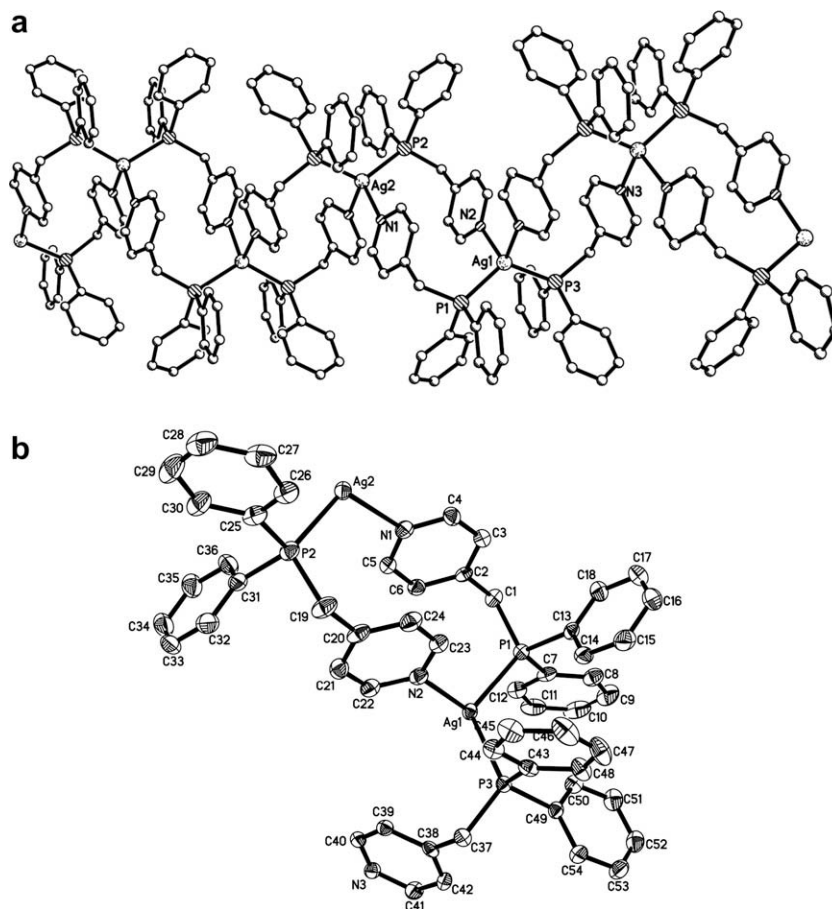


Fig. 4. (a) Ball-and-stick view of the extended cationic polymer of **3**. (b) Thermal ellipsoid of the unique cationic portion of **3** with an atomic numbering scheme. Ellipsoids are shown at the 50% level. Hydrogen atoms and two CH₃CN molecules have been removed for clarity.

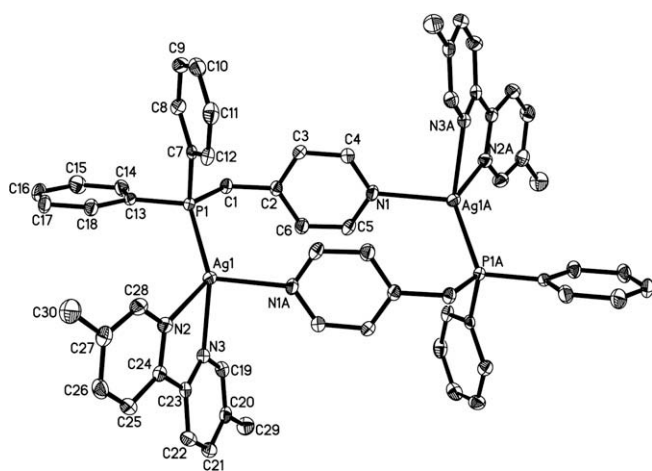


Fig. 5. Thermal ellipsoid plot of the cationic portion of **4** with an atomic numbering scheme. Ellipsoids are shown at the 50% level. Hydrogen atoms and two CH₂Cl₂ molecules have been removed for clarity.

the molecule through an inversion center, where the long bridging interaction between the Ag and O atoms are shown in dashed lines. The formation of **5** is independent of the ratio of reactants from which the reaction is carried out. Accordingly, a 3:2 ratio compound of PMP-41 and AgOtf is not feasible because of the coordinating ability of the Otf[−] ions to act either as a mono or bidentate ligand, when compared to the non-connectivity of the BF₄ anion. The metal centers in the molecular structure of **5** exhibit

a four-coordinate arrangement in a distorted tetrahedral geometry, due to the bridging interaction that distorts the symmetry of the angles. The Ag–P distance falls in the range of reported values, although the Ag–N distance (2.237(3) Å) corresponding to the pyridyl-metal contact is reported to be shorter when compared to the values in previous molecules discussed herein.

3.2.5. Structure of compound **6**

Compound **6** was obtained by addition of 1 equiv. of 5,5'-dimethyl-2,2'-bipyridine into a reaction mixture containing AgOtf and PMP-41 in a 1:1 ratio. The growth molecular structure of **6** is shown in Fig. 7a, and corresponds to the first example of the AgX/PMP-41 structures where the bimetallic box unit, commonly seen in these molecules, is disrupted by addition of an additional electron donating ligand. The unique portion of this structure is shown in Fig. 7b, and a view of the packing structure in Fig. S2. The extended view of the cationic portion of **6** (Fig. 7a) reveals a polymeric chain linked by PMP-41 ligands, displaying a zigzag conformation due to the reported angle of 110.5(2)° for C(2)–C(1)–P(1). The angles around the metal center describe a tetrahedron, slightly more distorted than in previous structures with N–Ag–N and P–Ag–N angles ranging from 70.41(10) to 118.95(8)° (Table 4). The aromatic rings of the bipyridine ligand are twisted from planarity at an angle of 16.5(1)°, probably due to the steric effects imparted by the phenyl rings of the PMP-41 ligands. The Otf anion in this instance acts non-coordinating, and is disordered about the position of the sulfur; therefore it was refined isotropically, and the two sulfur positions restrained to have the same thermal parameters.

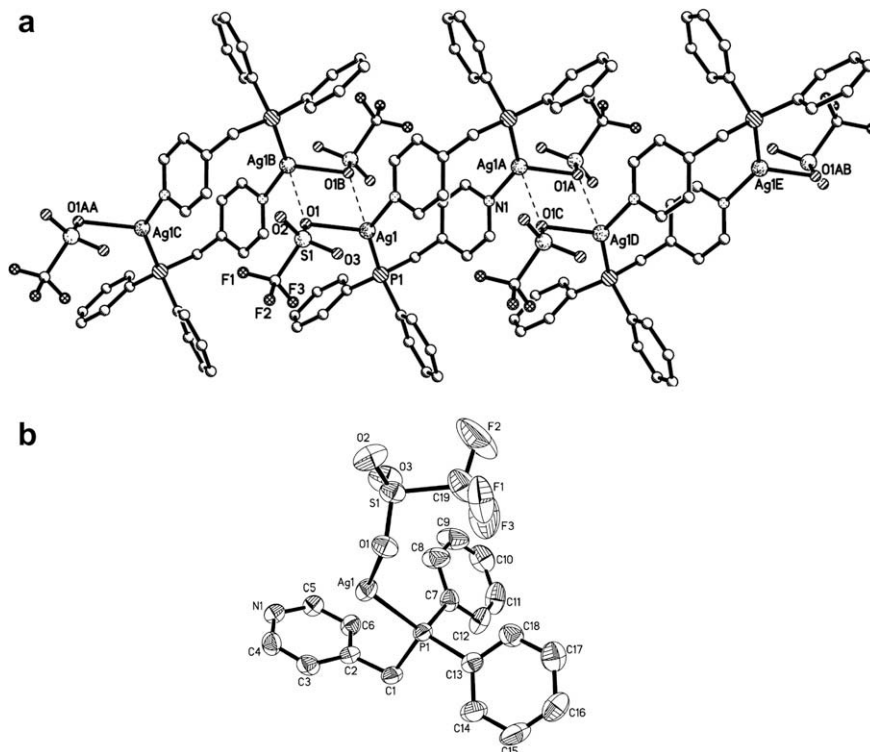


Fig. 6. (a) Ball-and-stick plot of the growth molecular structure of **5**. (b) Thermal ellipsoid of **5** with an atomic numbering scheme. Ellipsoids are shown at the 50% level. Hydrogen atoms have been removed for clarity.

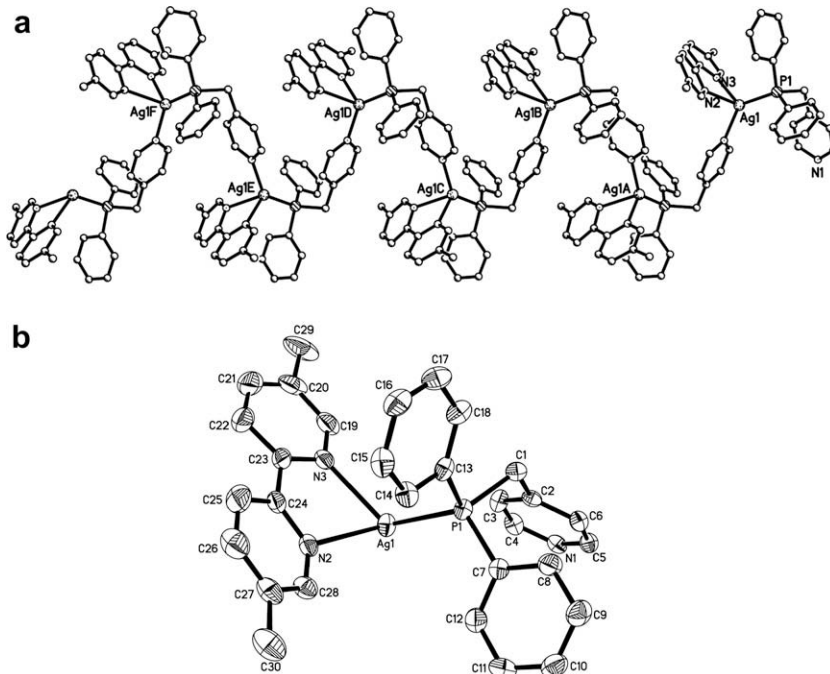


Fig. 7. (a) Expanded view of the two-dimensional growth of the cationic polymer of **6**. (b) Thermal ellipsoid plot of the unique cationic portion of **6** with an atomic numbering scheme. Ellipsoids are shown at the 50% level. Hydrogen atoms have been removed for clarity.

3.2.6. Structure of compound **7**

Compound **7** shown in Fig. 8 is obtained by addition of 1/2 equiv. of 4,4'-bipyridine to a reaction mixture containing a 1:1 ratio of PMP-41 ligand to AgOtf. The use of a bridging connector such as the 4,4'-bipyridine provides an extended coordination net-

work by linking together $[\text{AgOtf}(\text{PMP-41})_2]$ units through the Ag atoms (Fig. S3). The rings of the bipyridine ligand are highly twisted with an angle of $30.4(1)^\circ$, that results from the free rotation along the central C–C bond. The molecule presents three non-equivalent silver atoms, although each metal center displays

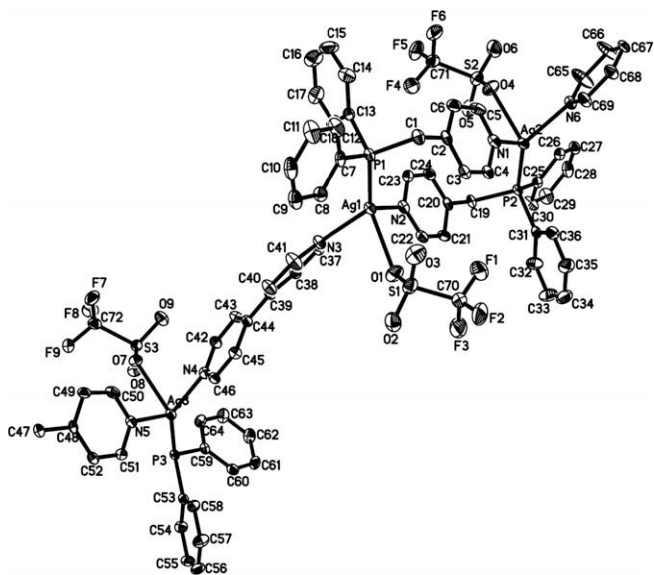


Fig. 8. Thermal ellipsoid plot of the unique portion of **7** with an atomic numbering scheme. Ellipsoids are shown at the 50% level. Hydrogen atoms have been removed for clarity.

the same connectivity of one P atom, one N from a PMP-41 ligand and one O atom of the coordinated Otf anion. Accordingly, the silver atoms are four-coordinated, where the angles around the metal centers describe a distorted tetrahedron for each Ag. All Ag–P, Ag–N, and Ag–O distances present little variances when moving from one silver atom to another, falling in the range of reported values. The center of the bimetallic box lies on a crystallographic inversion center.

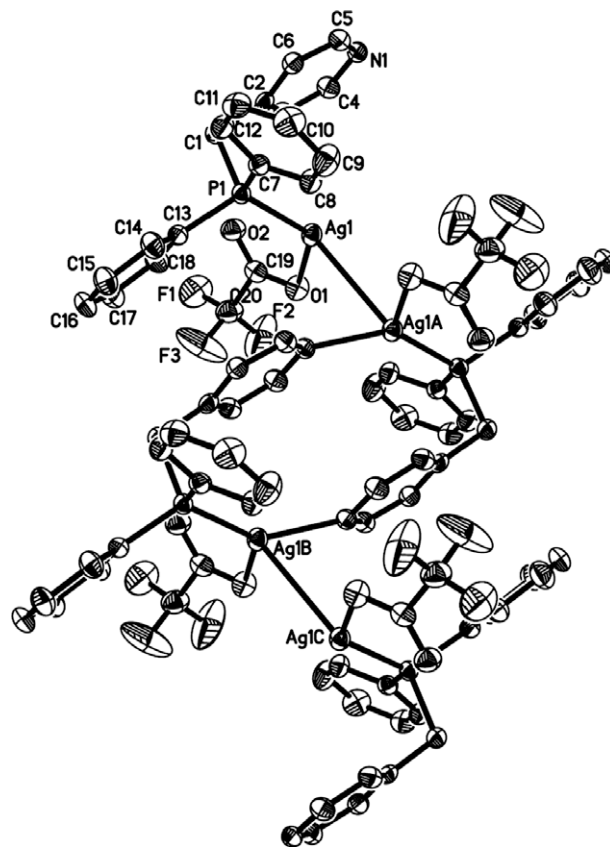


Fig. 9. Thermal ellipsoid of **8A** with an atomic numbering scheme. Ellipsoids are shown at the 50% level. Hydrogen atoms and a CH_3CN molecule have been removed for clarity.

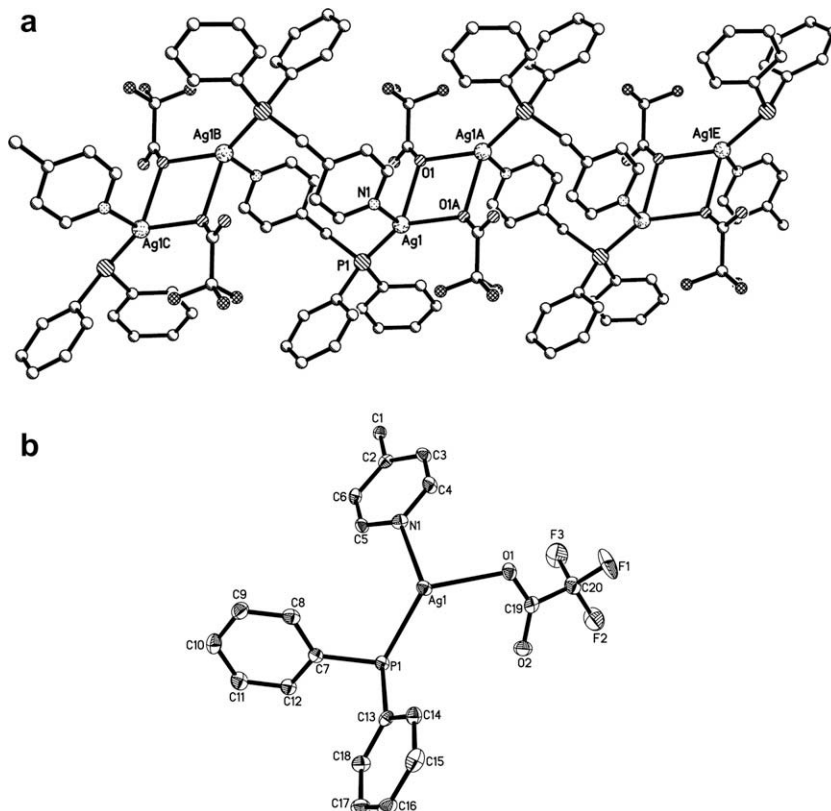


Fig. 10. (a) Ball-and-stick plot of the growth molecular structure of **8B**. (b) Thermal ellipsoid of the unique portion of **8B** with an atomic numbering scheme. Ellipsoids are shown at the 50% level. Hydrogen atoms have been removed for clarity.

Table 3

Selected bond lengths (Å), angles (°), and distances for the compounds [AgBF₄(PMP-41)(CH₃CN)₂]₂ (2), (AgBF₄)(PMP-41)₂ (3), [AgBF₄(PMP-41)(5,5'-dimethyl-2,2'-bipyridine)]₂ (4), and AgOtf(PMP-41) (5)^a

Compound 2			
Ag(1)–P(1)	2.3701(8)	Ag(1)–N(1)	2.304(2)
Ag(1)–N(2)	2.318(3)	Ag(1)–N(3)	2.394(3)
N(1)–Ag(1)–N(2)	94.04(10)	N(1)–Ag(1)–P(1)	121.72(6)
N(2)–Ag(1)–P(1)	125.55(8)	N(1)–Ag(1)–N(3)	106.74(9)
N(2)–Ag(1)–N(3)	89.96(11)	P(1)–Ag(1)–N(3)	113.21(7)
C(2)–C(1)–P(1)	110.54(19)		
Compound 3			
Ag(1)–P(1)	2.4600(9)	Ag(1)–P(3)	2.4667(8)
Ag(1)–N(2)	2.360(3)	Ag(1)–N(3)#1	2.343(3)
Ag(2)–P(2)	2.4465(9)	Ag(2)–P(2)#2	2.4465(9)
Ag(2)–N(1)	2.352(3)	Ag(2)–N(1)#2	2.352(3)
N(3)#1–Ag(1)–N(2)	103.16(9)	N(3)#1–Ag(1)–P(1)	106.90(7)
N(2)–Ag(1)–P(1)	110.67(7)	N(3)#1–Ag(1)–P(3)	111.25(6)
N(2)–Ag(1)–P(3)	101.32(7)	P(1)–Ag(1)–P(3)	121.95(3)
N(1)#2–Ag(2)–N(1)	101.28(13)	N(1)#2–Ag(2)–P(2)	99.74(7)
N(1)–Ag(2)–P(2)	115.11(7)	N(1)#2–Ag(2)–P(2)#2	115.11(7)
N(1)–Ag(2)–P(2)#2	99.74(7)	P(2)–Ag(2)–P(2)#2	124.20(4)
C(2)–C(1)–P(1)	110.4(2)	C(20)–C(19)–P(2)	110.1(2)
C(38)–C(37)–P(3)	112.7(2)		
Compound 4			
Ag(1)–P(1)	2.3523(6)	Ag(1)–N(1)#1	2.3850(16)
Ag(1)–N(2)	2.3363(16)	Ag(1)–N(3)	2.3444(15)
N(2)–Ag(1)–N(3)	71.58(5)	N(2)–Ag(1)–P(1)	127.29(4)
N(3)–Ag(1)–P(1)	133.61(4)	N(2)–Ag(1)–N(1)#1	102.34(6)
N(3)–Ag(1)–N(1)#1	95.06(6)	P(1)–Ag(1)–N(1)#1	116.27(4)
C(2)–C(1)–P(1)	110.98(12)		
Compound 5			
Ag(1)–P(1)	2.3564(9)	Ag(1)–N(1)#1	2.237(3)
Ag(1)–O(1)	2.489(2)		
N(1)#1–Ag(1)–P(1)	139.69(8)	N(1)#1–Ag(1)–O(1)	94.01(10)
P(1)–Ag(1)–O(1)	122.85(6)	C(2)–C(1)–P(1)	109.2(2)

^a Symmetry transformations used to generate equivalent atoms. For 2: #1 = -x + 1, -y + 2, -z. For 3: #1 = -x + 1, -y, -z + 1; #2 = -x + 2, y, -z + 3/2. For 4: #1 = -x + 1, -y + 2, -z + 1. For 5: #1 = -x, -y + 1, -z + 1.

3.2.7. Structure of compounds 8A and 8B

According to the molecular structures of **8A** and **8B**, the conformation of the PMP-41 ligand is seen to be quite sensitive to counterion effects due to the presence of a strong coordinating anion. In addition, the silver environment is just as susceptible, if not more so, to change when using different crystallization solvent systems. The molecular structure shown in Fig. 9 was obtained by layering ether into a solution of compound **8** in CH₃CN, while in Fig. 10b is shown the thermal ellipsoid of **8B**, formed by layering ether into a solution of compound **8** in DMF. Both correspond to polymeric structures displaying notable differences in connectivity even when they were obtained by using the same starting materials. The crystal structure of **8A** displays an uncommon Ag–Ag interaction for compounds involving the bidentate PMP-41 ligand. The structure conserves the same bimetallic box conformation observed in the other compounds, where the infinite chain is supported by the metal–metal interactions with a distance of 3.1084(6) Å that falls in the range of reported values. The metal center displays a distorted tetrahedral geometry, bound to a P and a N atom of two different PMP-41 ligands, an O from the tfa anion, and the already mentioned Ag–Ag bond. The metallophilic interaction only observed in this structure is probably favored by the electronegative effect imparted by the O atom of the tfa anion, which is better stabilized by a metal–metal interaction than by the electronic contribution from a pyridyl group of another PMP-41 ligand. The crystal structure of compound **8B** reveals a diamond like binuclear silver center with each Ag bridged by two tfa⁻ ions. This type of conformations has been reported before in our group when oxygen-containing counteranions were used [47,48]. The 4-center bimetallic interaction exhibit an approximate separation

Table 4

Selected bond lengths (Å), angles (°), and distances for the compounds AgOtf(PMP-41)(5,5'-dimethyl-2,2'-bipyridine) (6), [AgOtf(PMP-41)](4,4'-bipyridine)_{1/2} (7), and Agtfa(PMP-41) (8)^a

Compound 6			
Ag(1)–P(1)	2.3771(9)	Ag(1)–N(1)#1	2.280(3)
Ag(1)–N(2)	2.412(3)	Ag(1)–N(3)	2.362(3)
N(1)#1–Ag(1)–N(3)	101.82(10)	N(1)#1–Ag(1)–P(1)	70.41(10)
N(3)–Ag(1)–P(1)	118.95(8)	N(1)#1–Ag(1)–N(2)	100.27(10)
N(3)–Ag(1)–N(2)	70.41(10)	P(1)–Ag(1)–N(2)	109.59(7)
C(2)–C(1)–P(1)	110.5(2)		
Compound 7			
Ag(1)–P(1)	2.3647(9)	Ag(1)–N(2)	2.347(3)
Ag(1)–N(3)	2.323(3)	Ag(1)–O(1)	2.456(2)
Ag(2)–P(2)	2.3579(9)	Ag(2)–N(1)	2.347(3)
Ag(2)–N(6)	2.304(3)	Ag(2)–O(4)	2.454(2)
Ag(3)–P(3)	2.3639(9)	Ag(3)–N(4)	2.289(3)
Ag(3)–N(5)	2.356(2)	Ag(3)–O(7)	2.522(2)
N(3)–Ag(1)–N(2)	96.58(9)	N(3)–Ag(1)–P(1)	128.07(7)
N(2)–Ag(1)–P(1)	121.61(7)	N(3)–Ag(1)–O(1)	80.49(9)
N(2)–Ag(1)–O(1)	86.88(9)	P(1)–Ag(1)–O(1)	130.45(6)
N(6)–Ag(2)–N(1)	94.84(9)	N(6)–Ag(2)–P(2)	133.96(7)
N(1)–Ag(2)–P(2)	125.84(7)	N(6)–Ag(2)–O(4)	83.33(9)
N(1)–Ag(2)–O(4)	87.91(9)	P(2)–Ag(2)–O(4)	115.14(6)
N(4)–Ag(3)–N(5)	91.02(9)	N(4)–Ag(3)–P(3)	141.64(7)
N(5)–Ag(3)–P(3)	123.22(7)	N(4)–Ag(3)–O(7)	82.76(8)
N(5)–Ag(3)–O(7)	87.87(8)	P(3)–Ag(3)–O(7)	112.48(5)
C(2)–C(1)–P(1)	110.3(2)	C(20)–C(19)–P(2)	110.0(2)
C(48)–C(47)–P(3)#1	110.2(2)		
Compound 8A			
Ag(1)–Ag(1)#2	3.1084(6)	Ag(1)–P(1)	2.3743(9)
Ag(1)–N(1)#1	2.262(3)	Ag(1)–O(1)	2.359(2)
N(1)#1–Ag(1)–O(1)	93.17(9)	N(1)#1–Ag(1)–P(1)	137.87(7)
O(1)–Ag(1)–P(1)	125.18(6)	N(1)#1–Ag(1)–Ag(1)#2	65.20(7)
O(1)–Ag(1)–Ag(1)#2	79.31(6)	P(1)–Ag(1)–Ag(1)#2	132.11(2)
C(2)–C(1)–P(1)	108.4(2)		
Compound 8B			
Ag(1)–P(1)	2.3630(9)	Ag(1)–N(1)	2.343(3)
Ag(1)–O(1)	2.408(2)	Ag(1)–O(1)#1	2.401(2)
N(1)–Ag(1)–P(1)	116.29(7)	N(1)–Ag(1)–O(1)#1	87.77(9)
P(1)–Ag(1)–O(1)#1	146.42(6)	N(1)–Ag(1)–O(1)	90.51(9)
P(1)–Ag(1)–O(1)	125.34(5)	O(1)#1–Ag(1)–O(1)	73.91(8)
C(2)–C(1)–P(1)#2	111.0(2)		

^a Symmetry transformations used to generate equivalent atoms. For 6: #1 = -x + 3/2, y - 1/2, -z + 1/2; #2 = -x + 3/2, y + 1/2, -z + 1/2. For 7: #1 = -x + 3, -y - 1, -z; #2 = -x, -y + 1, -z + 1. For 8A: #1 = -x + 1, -y + 1, -z + 1; #2 = -x, -y + 1, -z + 1. For 8B: #1 = -x + 1/2, -y + 5/2, -z; #2 = -x + 1/2, -y + 3/2, -z.

of 90° with respect to the plane of the bimetallic box, thus resulting in a polymeric structure with a zigzag conformation (Fig. 10a). The silver atoms have a distorted tetrahedral geometry with a Ag1–Ag1A distance of 3.8686(9) Å. Each Ag is also bound to two phosphine ligands with opposing ends facing each other in a head-to-tail fashion, as observed in all other AgX/PMP-41 structures. The Ag(1)–O(1)#1 distance displays a value of 2.401(2) Å, which is longer than the observed in compound **8A** with a value of 2.359(2) Å, due to weaker interactions when the O atom displays a bridging mode.

3.3. Luminescence properties

Self-assembled coordination complexes that present high luminous efficiency are currently of great interest due to their potential in microelectronics, sensor technologies, non-linear optics, porous materials, and other applications [48–53]. Organometallic complexes associated with ligands that contain aromatic nitrogen heterocycles have been extensively studied as they can be used as light-emitting devices. According to this, the absorption and emission properties of these materials may be adjusted by varying the metal environment and employing ligands that can effectively enhance luminescence properties. In this work, can be seen dra-

Table 5
Luminescent spectral data for compounds **2–8** at 77 K and 1×10^{-4} M in CH_3CN

Compound	Excitation λ_{max} (nm)	Emission local λ_{min} (nm)
2	393, 408	283, 288
3	398, 418	289
4	448, 481	318
5	382, 393	279
6	446, 473	314
7	412, 438, 462	297
8	387, 396	282

matic changes in the luminescence properties of the metal complexes by introducing in the coordination sphere of the metal additional electron donating ligands, as they are the 5,5'-dimethyl-2,2'-bipyridine and the 4,4'-bipyridine. Here we report the excitation and emission spectra of the metal complexes; all spectra were recorded at concentrations of 1×10^{-4} M in acetonitrile glasses at 77 K, and shown in Figs. S4 and S5.

According to the intensity of the emission and excitation maxima of the compounds discussed herein, these can be separated into two groups. Molecules that present only metal-PMP-41 interactions and metal complexes obtained by adding 5,5'-dimethyl-2,2'-bipyridine or 4,4'-bipyridine to reaction mixtures containing AgX/PMP-41 , which show a clear difference in intensity of the emission and excitation spectra. Excitation maxima of all compounds are presented in Table 4 along with the local emission maxima. Excitation maxima for **2**, **3**, **5** and **8** are 283, 289, 279 and 282 nm, respectively, with intensities that reach up to the 4.2×10^6 cps units. As expected the excitation spectra of these compounds are very similar, given the same structural conformation of the phosphine ligand with the silver metal in the complexes. The emission spectra of the mentioned compounds show two maximums for each case, illustrating the decay transitions associated with each system, and covering a small range of the spectrum with local maxima that range between 283 and 289 nm. Comparing the emission data of the compounds based on the AgBF_4 salt, a red shift of the maximum of approximately 30 nm is observed for the $[\text{AgBF}_4(\text{PMP-41})_2]$ complex with respect to the same compound coordinated to the 5,5'-dimethyl-2,2'-bipyridine. The same luminescent behavior is observed for the series of compounds obtained with the AgOtf salt, where the maximum in the emission spectrum of the $\text{AgOtf}(\text{PMP-41})$ compound is red shifted with respect to compounds **6** and **7**. However, the most noticeable difference between the $[\text{AgX}(\text{PMP-41})_2]$ compounds and their corresponding analogous coordinated to either the 5,5'-dimethyl-2,2'-bipyridine or 4,4'-bipyridine, is the increased intensity in which the latter group of compounds emit, observing differences up to 1×10^6 units of cps. This high luminescent efficiency of compounds containing bipyridine type ligands have been reported before [54,55], particularly in complexes of some transition metals of the group VII and VIII, where the metal-bipyridine interactions illustrates the complexity of the decay transitions associated with the more complicated system.

4. Conclusions

We have reported the synthesis of a novel pyridyl containing phosphine, which shows the ability to bind silver ions through both the phosphorus and nitrogen moieties. Several new coordination polymers and discrete molecules of Ag(I) have been characterized using X-ray crystallography, which reveals a structure dependence on the anion and the solvent system used for crystallization. Reaction of the 5,5'-dimethyl-2,2'-bipyridine and 4,4'-bipyridine ligands with AgX/PMP-41 adducts results in the formation of extended polymeric networks, conserving most of the time

the bimetallic box conformation of the PMP-41 structures. The complexes, according to their structures and luminescent characteristics, are seen to be highly dependent on the bipyridine ligand used in the reaction, which is also responsible for the enhancement of the excitation and emission spectra intensities. To date, we are continuing to study the coordination properties of **1** with other metals and are also actively pursuing the bisubstituted pyridyl PMP-42 ligand. Studies of phosphine-substituted ligands of the type $\text{PPh}_x\text{CH}_2\text{py}_{3-x}$ ($x = 0, 1, 2$) will be continued, as well as substituted and non-substituted bipyridines in mixed ligand systems.

Acknowledgements

This research was supported by funds provided by a Grant from the Robert A. Welch Foundation (AA-1508). The Bruker X8 APEX diffractometer was purchased with funds received from the national Science Foundation Major Research Instrumentation Program Grant CHE-0321214.

Appendix A. Supplementary data

CCDC 682322, 680324, 680327, 680320, 680325, 680326, 680321 and 680323 for contain the supplementary crystallographic data for **2**, **3**, **4**, **5**, **6**, **7**, **8A** and **8B**. These data can be obtained free of charge from the Cambridge Crystallographic Data Centre via www.ccdc.cam.ac.uk/data_request/cif. Supplementary data associated with this article can be found, in the online version, at doi:10.1016/j.ica.2008.04.032.

References

- [1] P. Espinet, K. Soulantica, *Coord. Chem. Rev.* 193 (1999) 499.
- [2] G.R. Newkome, *Chem. Rev.* 93 (1993) 2067.
- [3] V.F. Slagt, P.W.N.M. van Leeuwen, J.N.H. Reek, *Chem. Commun.* (2003) 2474.
- [4] Z.Z. Zhang, H. Cheng, *Coord. Chem. Rev.* 147 (1996) 1.
- [5] G.R. Newkome, D.C.J. Hager, *Org. Chem.* 43 (1978) 947.
- [6] M. Kuil, P.E. Goudriaan, P.W.N.M. van Leeuwen, J.N.H. Reek, *Chem. Commun.* (2006) 4679.
- [7] X.B. Jiang, L. Lefort, P.E. Goudriaan, A.H.M. de Vries, P.W.N.M. van Leeuwen, J.G. de Vries, J.N.H. Reek, *Angew. Chem., Int. Ed.* 45 (2006) 1223.
- [8] J.N.H. Reek, M. Roder, P.E. Goudriaan, P.C.J. Kamer, P.W.N.M. van Leeuwen, V.F.J. Slagt, *Organomet. Chem.* 690 (2005) 4505.
- [9] V.F. Slagt, M. Roder, P.C.J. Kamer, P.W.N.M. van Leeuwen, J.N.H. Reek, *J. Am. Chem. Soc.* 126 (2004) 4056.
- [10] V.F. Slagt, P.C.J. Kamer, P.W.N.M. van Leeuwen, J.N.H. Reek, *J. Am. Chem. Soc.* 126 (2004) 1526.
- [11] A. Buhling, P.C.J. Kamer, P.W.N.M. van Leeuwen, J.W. Elgersma, *J. Mol. Catal. A: Chem.* 116 (1997) 297.
- [12] A. Buhling, P.C.J. Kamer, P.W.N.M. van Leeuwen, *J. Mol. Catal. A: Chem.* 98 (1995) 69.
- [13] E. Drent, P. Arnoldy, P.H.M. Budzelaar, *J. Organomet. Chem.* 455 (1993) 247.
- [14] E. Drent, P. Arnoldy, P.H.M. Budzelaar, *J. Organomet. Chem.* 475 (1994) 57.
- [15] A. Hassner, L.R. Krepski, V. Alexanian, *Tetrahedron* 34 (1978) 2069.
- [16] E. De la Encarnacion, J. Pons, R. Yanez, J. Ros, *Inorg. Chim. Acta* 359 (2006) 745.
- [17] A. Murso, D. Stalke, *Z. Anorg. Allg. Chem.* 630 (2004) 1025.
- [18] A. Aegy, G. Consiglio, *Inorg. Chim. Acta* 296 (1999) 45.
- [19] P. Braunstein, B.T. Heaton, C. Jacob, L. Manzi, X. Morise, *Dalton Trans.* (2003) 1396.
- [20] F. Hung-Low, K.K. Klausmeyer, *Inorg. Chim. Acta* 361 (2008) 1298.
- [21] E. Lindner, H. Rauleder, W. Hiller, *Z. Naturforsch. B: Anorg. Chem., Org. Chem.* 4 (1983) 417.
- [22] K.K. Klausmeyer, F. Hung, *Acta Crystallogr. Sect. E: Struct. Rep.* E62 (2006) m2415.
- [23] C. Janiak, *J. Chem. Soc., Dalton Trans.* (2000) 3885.
- [24] D. Sun, R. Cao, Y. Sun, W. Bi, X. Li, Y. Wang, Q. Shi, X. Li, *Inorg. Chem.* 42 (2003) 7512.
- [25] R.P. Feazell, C.E. Carson, K.K. Klausmeyer, *Inorg. Chem.* 45 (2006) 935.
- [26] R.P. Feazell, C.E. Carson, K.K. Klausmeyer, *Inorg. Chem.* 45 (2006) 2627.
- [27] R.P. Feazell, C.E. Carson, K.K. Klausmeyer, *Inorg. Chem.* 45 (2006) 2635.
- [28] M.A. Weiner, P. Schwartz, *Inorg. Chem.* 14 (1975) 1714.
- [29] I. Angurell, O. Rossell, M. Seco, E. Ruiz, *Organometallics* 24 (2005) 6365.
- [30] E.C. Carson, S.J. Lippard, *J. Am. Chem. Soc.* 126 (2004) 3412.
- [31] L. Hirsivaara, M. Haukka, J. Pursiainen, *J. Organomet. Chem.* 633 (2001) 66.
- [32] C. Kaes, A. Katz, M.W. Hosseini, *Chem. Rev.* 100 (2000) 3553.

- [33] H.L. Zhu, Q. Chen, W.L. Peng, S.J. Qi, A.L. Xu, X.M. Chen, *Chin. J. Chem.* 19 (2001) 263.
- [34] K. Biradha, M. Sarkar, L. Rajput, *Chem. Commun.* (2006) 4169.
- [35] S.A. Barnett, N.R. Champness, *Coord. Chem. Rev.* 246 (2003) 145.
- [36] L.C. Silva, R. Ahmad, M.J. Carr, A. Franken, J.D. Kennedy, M.J. Hardie, *Cryst. Growth Des.* 7 (2007) 658.
- [37] H.W. Park, S.M. Sung, ; K.S. Min, H. Bang, M.P. Suh, *Eur. J. Inorg. Chem.* (2001) 2857.
- [38] Bruker. APEX2 (Version 2. 0) and SAINT-Plus (Version 6. 25), Bruker AX Inc., Madison, Wisconsin, USA, 2003.
- [39] G.M. Sheldrick, *SHELXS97* and *SHELXL97*. University of Gottingen, Germany, 1997.
- [40] G.M. Sheldrick, *SHELXTL* (Version 6.10). Bruker AXS Inc., Madison, Wisconsin, USA, 2000.
- [41] A.L. Spek, *PLATON-90*. *Acta Crystallogr.* A46, C34. A Multipurpose Crystallographic Tool, University of Utrecht, The Netherlands, 2006.
- [42] C. Jia, S.X. Liu, A. Neels, G. Labat, S. Decurtins, *Polyhedron* 24 (2005) 3032.
- [43] D.J. Eisler, R.J. Puddephatt, *Inorg. Chem.* 44 (2005) 4666.
- [44] L. Lettko, J.S. Wood, M.D. Rausch, *Inorg. Chim. Acta* 308 (2000) 37.
- [45] G.A. Van Albada, W.J.J. Smeets, A.L. Spek, J. Reedijk, *Inorg. Chim. Acta* 260 (1997) 151.
- [46] K.A. Hirsch, S.R. Wilson, J.S. Moore, *Inorg. Chem.* 36 (1997) 2960.
- [47] K.K. Klausmeyer, R.P. Feazell, J.H. Reibenspies, *Inorg. Chem.* 43 (2004) 1130.
- [48] R.P. Feazell, C.E. Carson, K.K. Klausmeyer, *Inorg. Chem.* 44 (2005) 996.
- [49] V.W.W. Yam, K.K.W. Lo, *Chem. Soc. Rev.* 28 (1999) 323.
- [50] Y. Zhou, X. Zhang, W. Chen, H. Qiu, *J. Organomet. Chem.* 693 (2008) 205.
- [51] T.S. Teets, D.V. Partyka, A.J. Esswein, J.B. Updegraff, M. Zeller, A.D. Hunter, T.G. Gray, *Inorg. Chem.* 46 (2007) 6218.
- [52] D. Song, S. Wang, *Eur. J. Inorg. Chem.* (2003) 3774.
- [53] R.P. Feazell, C.E. Carson, K.K. Klausmeyer, *Eur. J. Inorg. Chem.* (2005) 3287.
- [54] Y. Ma, Y. He, L. Zhang, X. Wang, J. Gao, Z. Han, *Struct. Chem.* 18 (2007) 1005.
- [55] Z. Guo, X. Li, S. Gao, Y. Li, R. Cao, *J. Mol. Struct.* 846 (2007) 123.